IV Escola de Primavera de Transição e Turbulência
Universidade Federal do Rio Grande do Sul
Pontifícia Universidade Católica do Rio Grande do Sul
Porto Alegre, RS, 27 de setembro a 1º de outubro de 2004

NUMERICAL SIMULATION OF FLOWS OVER CILYNDERS USING THE IMMERSED BOUNDARY METHOD

Alice Rosa da Silva
Federal University of Uberlândia – UFU, School of Mechanical Engineering, Av. João Naves de Ávila 2160, Uberlândia - MG
arsilva@mecanica.ufu.br

Gustavo Bifaroni de Carvalho
Estadual University Paulista, School of Engineering of Ilha Solteira, Ilha Solteira - SP
bifaroni@dem.feis.unesp.br

Ana Lúcia Fernandes de Lima e Silva
Federal University of Uberlândia – UFU, School of Mechanical Engineering, Av. João Naves de Ávila 2160, Uberlândia - MG
alfsilva@mecanica.ufu.br

Sérgio Said Mansur
Estadual University Paulista, School of Engineering of Ilha Solteira, Ilha Solteira - SP
mansur@dem.feis.unesp.br

Aristeu da Silveira Neto
Federal University of Uberlândia – UFU, School of Mechanical Engineering, Av. João Naves de Ávila 2160, Uberlândia - MG
aristeus@mecanica.ufu.br

Abstract. *In the present work, the Immersed Boundary Method (Peskin, 1977) with the Virtual Physical Model-VPM (Lima e Silva et al., 2003) was employed to simulate incompressible and two-dimensional flows over cylindrical geometries. This methodology uses two type of grids, one Eulerian-Cartesian to represent the flow and one Lagrangean to represent the immersed body. The first grid is fixed and the second can move. Simulations were carried out over stationary and rotating cylinders at different Reynolds numbers and for several values of specific rotation. The Smagorinsky turbulence model and a smooth function were used in order to have a numerically stable methodology. The drag and the lift coefficients, the Strouhal number and surfaces of vorticity were obtained and compared with others authors.*

Keywords*. Immersed Boundary Method, stationary cylinder, moving cylinder*

1. Introduction

The immersed boundary methodology, developed by Peskin (1977), was used in the present work. Several authors have used and developed this methodology to simulate flows over different kind of immersed bodies. Fogelson and Peskin (1988) studied the phenomena of plaquet aggregation during the blood flow. The numerical method developed was an extension of the Peskin's method. Goldstein *et al*. (1993) used the spectral method to simulate flows over cylinders at low Reynolds number. The model presented by authors to calculate the force field in the Lagrangean grid, has two adjustable constants. Saiki and Biringen (1996) used the immersed boundary methodology to simulate flows over mobile and stationary cylinders at low Reynolds number ($Re \leq 400$). The authors used the model proposed by Goldstein *et al*. (1993), to calculate the force field inherent to this methodology. Lima e Silva (2002) and Lima e Silva *et al*. (2003) developed the Virtual Physical Model to calculate the Lagrangean interfacial force. This model is based in the Navier-Stokes equations for fluid volumes centered in the Lagrangean points, which are placed over fluid-solid interface.

Attention of many authors has been given to control the shedding vortex behind cylinders. Koopmann (1967) investigated experimentally the effect of the forced vibration induced by the fluid over a circular cylinder, to low Reynolds numbers. Tuszynski e Lönher (1998) analyzed by numerical simulations, the effect of rotation of a circular cylinder in the drag force. Carvalho (2003) has investigated experimentally flows over rotating cylinder.

The group of fluid dynamics LTCM/UFU (Laboratory of Heat and Mass Transfer and Fluid Dynamic) has been worked to develop the immersed boundary methodology for flows over complex and mobile geometries. In the present work the authors present the development and application of this methodology to stationary and rotating cylinders. In the first case (stationary cylinders), vortices are formed behind the cylinders to Reynolds numbers greater than the critical value. In the second case (rotating cylinders), the vortices are displaced with respect to the symmetry plane. The results of the present work were compared with results of other authors.

2. Mathematical Model

The Immersed Boundary Method uses the Navier-Stokes equations and mass conservation to simulate incompressible and two-dimensional flow over stationary and rotating cylinders. The Navier-Stokes equations can be written as follow:

$$\frac{\partial u_i}{\partial t} + \frac{\partial \left(u_i u_j\right)}{\partial x_j} = -\frac{1}{\rho}\frac{\partial p}{\partial x_i} + \frac{\partial}{\partial x_j}\left[\nu\left(\frac{\partial u_i}{\partial x_j} + \frac{\partial u_j}{\partial x_i}\right)\right] + f_i\,, \tag{1}$$

$$\frac{\partial u_i}{\partial x_i} = 0\,, \tag{2}$$

where ρ and ν are the fluid density and the fluid cinematic viscosity, respectively, p is the pressure and u_i is the i component of the velocity. The Eulerian force field f_i, in the Eq. (1), models the immersed boundary. This force is calculated by the distribution of the Lagrangean force components, $\vec{F}(\vec{x}_k, t)$, by equation:

$$\vec{f}(\vec{x}) = \sum_k D_{ij}(\vec{x} - \vec{x}_k)\vec{F}(\vec{x}_k)\Delta s^2(\vec{x}_k), \tag{3}$$

where $\vec{x}$ and $\vec{x}_k$ are the position vectors of the Eulerian and Lagrangean points, $\Delta s(\vec{x}_k)$ is the length between two Lagrangean points, D_{ij} is a interpolation/distribution function and the $\vec{F}(\vec{x}_k)$ is the interfacial force calculated by the Virtual Physical Model (VPM) presented as follow:

$$\vec{F}(\vec{x}_k, t) = \rho\frac{\partial \vec{V}(\vec{x}_k, t)}{\partial t} + \rho\vec{\nabla}.\left(\vec{V}(\vec{x}_k, t)\vec{V}(\vec{x}_k, t)\right) - \mu\nabla^2\vec{V}(\vec{x}_k, t) + \vec{\nabla}p(\vec{x}_k, t)\,, \tag{4}$$

where the terms of Eq. (4) are denominated as acceleration force $\vec{F}_a$, inertial force $\vec{F}_i$, viscous force $\vec{F}_v$ and pressure force $\vec{F}_p$, respectively. After the determination of the Lagrangean force, it is distributed to Eulerian grid by Eq. (3).

In order to simulate high Reynolds numbers, the Navier-Stokes equation are filtered using a box filter imposed by the numerical grid used to the discretization process (Silveira-Neto, 2003). The formal filtered Navier-Stokes equations are written as follow:

$$\frac{\partial \overline{u}_i}{\partial t} + \frac{\partial \left(\overline{u_i u_j}\right)}{\partial x_j} = -\frac{1}{\rho}\frac{\partial \overline{p}}{\partial x_i} + \frac{\partial}{\partial x_j}\left[\nu\left(\frac{\partial \overline{u}_i}{\partial x_j} + \frac{\partial \overline{u}_j}{\partial x_i}\right)\right] + f_i\,, \tag{5}$$

$$\frac{\partial \overline{u}_i}{\partial x_i} = 0\,. \tag{6}$$

Defining a global sub-grid stress tensor, as proposed by Germano (1991), we rewrite Eq. (5) as the turbulence global equations:

$$\frac{\partial \overline{u}_i}{\partial t} + \frac{\partial \left(\overline{u}_i \overline{u}_j\right)}{\partial x_j} = -\frac{1}{\rho}\frac{\partial \overline{p}}{\partial x_i} + \frac{\partial}{\partial x_j}\left[\nu\left(\frac{\partial \overline{u}_i}{\partial x_j} + \frac{\partial \overline{u}_j}{\partial x_i}\right) + \tau_{ij}\right] + f_i\,, \tag{7}$$

where $\tau_{ij} = -\left(\overline{u_i u_j} - \overline{u}_i \overline{u}_j\right)$ is the sub-grid Reynolds stress tensor. Details of this filtering process can be found in Silveira-Neto *et al*. (2002) and Silveira-Neto (2003). The Smagorinsky (1963) sub-grid scale turbulence model was employed, in which the turbulent viscosity is calculated using the relation $\nu_t = (C_S \ell)^2\sqrt{2\overline{S}_{ij}\overline{S}_{ij}}$. The Smagorinsky constant was fixed as $C_s = 0.18$ and $\ell = \sqrt{\Delta x \Delta y}$.

3. Numerical methodology

The fractional step method with staggered grid was used to coupling pressure and velocity fields. The spatial discretization was performed with the central difference method and the time discretization with the second order Adams-Bashforth scheme. The discretization of the Navier-Stokes equations was made explicitly to velocity component and a linear system was solved, at each iteration, to the pressure correction. This method consists to estimate the velocity field, based in the fields of pressure, velocity and force of the previous iteration. In the next step the pressure field correction is determined and the new field of velocity, that satisfy the mass conservation, is finally calculated. The

velocity field is calculated explicitly while the pressure field is calculated solving a linear system of equations. The MSI solver (Schneider and Zedan, 1981) is used.

The Adams-Bashforth second order scheme is used in this paper for the time evolution and the details about this scheme can be found in Silva (2004).

4. Results

Results for stationary cylinder will be firstly presented. The simulations were carried out at different Reynolds number, using a grid of *125 x 250* points. The flow develops in the ascendant direction. Figure (1) shows the domain and the geometrical parameters used in the present simulations.

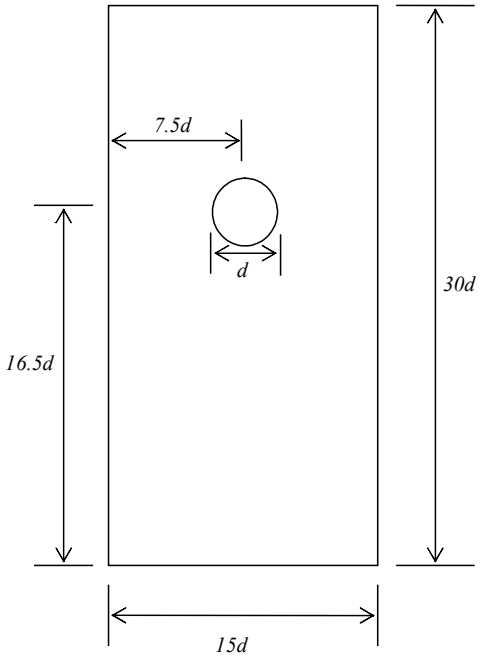

Figure 1. Illustrating scheme of the calculation domain.

4.1. Simulations with stationary cylinder

Figure 2 shows the flow visualization for different values of Reynolds number. The vorticity surfaces are visualized. The second order Adams-Bashforth scheme was used. In these simulations, no sub-grid turbulence model was used.

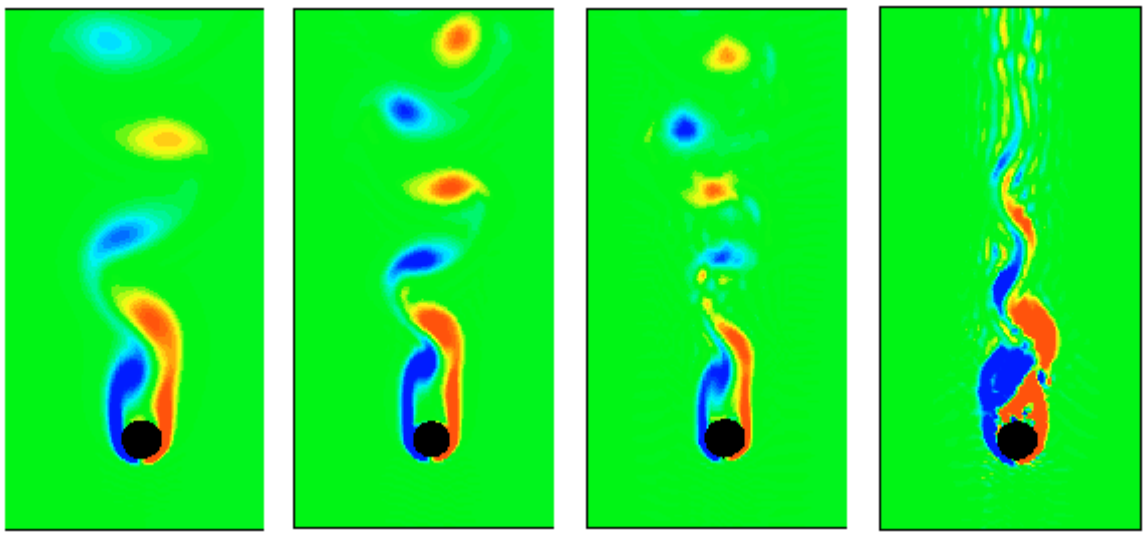

(a) (b) (c) (d)

Figure 2. Surfaces of vorticity: (a) *Re = 100*; (b) *Re = 300*; (c) *Re = 1000*. and (d) *Re = 10000*

Note that as the Reynolds number increases, numerical instabilities appear in the flow, as can be visualized in Figs. (2c) and (2d). These instabilities are expected once these simulations were performed without turbulence model. The spatial discretization (central difference scheme) has no numerical diffusion, and then it is natural that the simulation diverges.

Figure 3 shows the time evolution of the drag coefficient at Reynolds numbers equals to *100, 300, 1000* and *10000*, where the instabilities can be clearly visualized for *Re* equal to *1000* and *10000*.

The turbulence model (Smagorinsky, 1963) was used to control these instabilities. Figure 4, shows the flow visualization by surfaces of vorticity. The Reynolds number is equals to *1000* and *10000*. The same Cartesian grid was used.

Comparing Figs. (2c) and (4a) we see that the flow becomes more stable with the use of turbulence model. Nevertheless, for Reynolds number equal to *10000* (Fig. 4b), these instabilities appear again. Our numerical experiments show that the use of a smoothing function (Souza *et al.*, 2000) together with the turbulence model gives more stable results, as will be shown in the next section.

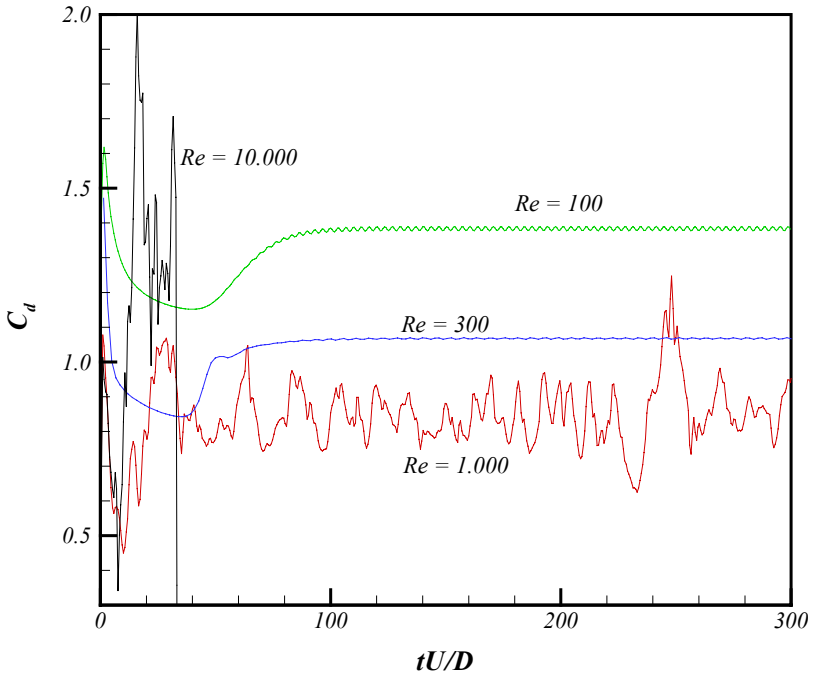

Figure 3. Time evolution of drag coefficient at Reynolds number equals to *100, 300*, *1000* and *10000* – calculations without turbulence model.

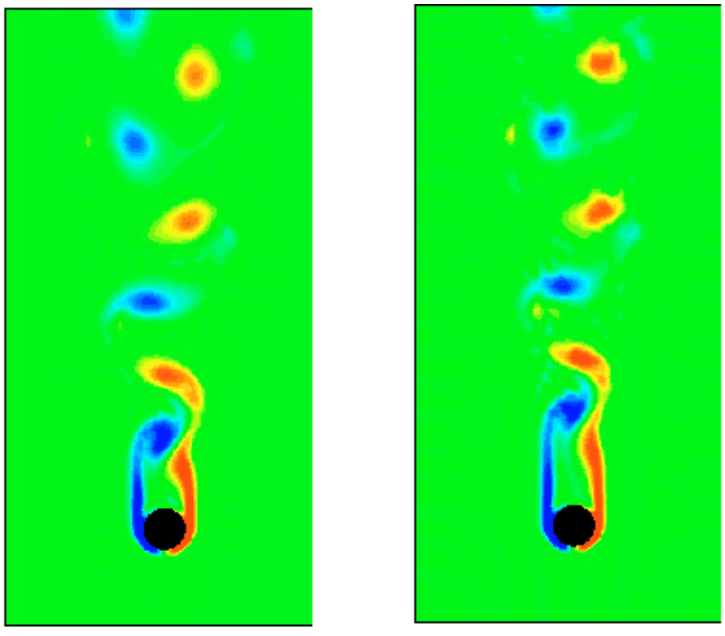

(a) (b)

Figure 4. Surfaces of vorticity at Reynolds number equal to (a) *1000* and (b) *10000*, both with turbulence model.

Figure 5 shows the C_d time distribution for *Re=1000* and *Re=10000*, with and without turbulence model. We see that both time distributions without turbulence models present excessive oscillations showing numerical divergence. Otherwise, both time distributions, with turbulence model, are stable and very regular. This shows that, nevertheless the numerical oscillations shown in Fig. 4 (b), the drag coefficient is well calculated.

Figure 6a shows that the vortex wake that is formed behind the cylinder is not aligned over the vertical symmetry plan, as expected. It is clearly that at the outlet of the domain there is a numerical instability with mass being transported inside of the domain. In order to control this kind of instability a smoothing function has been used to dump the vortex at the outlet of the domain. This function is well described at Silva (2004). The simulations shown in Figs. (6b) and (6c) were performed using the turbulence model and the smoothing function. We see that the numerical instability are better controlled and that, in both cases, the vortex streets are aligned in the vertical direction.

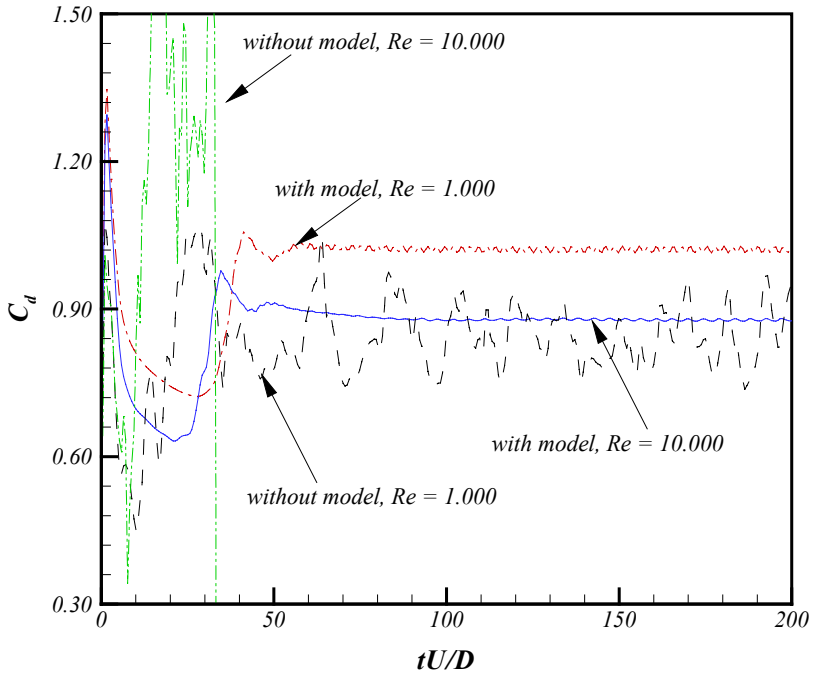

Figure 5. Time evolution of drag coefficient at *Re = 1000* and *Re = 10000*, *125 x 250* points.

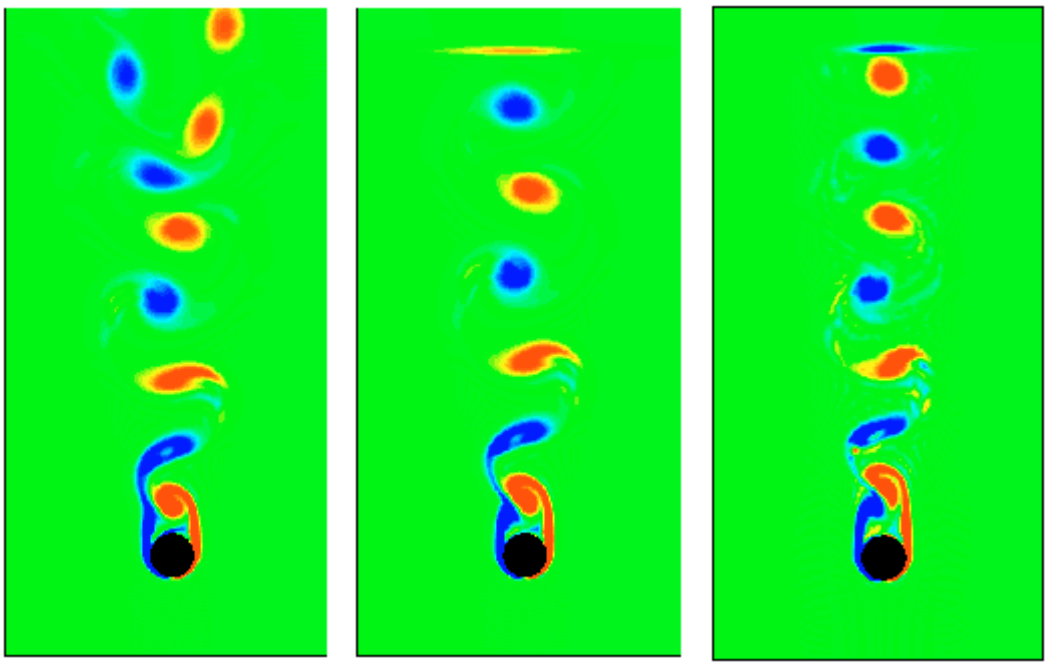

(a) (b) (c)

Figure 6. Surfaces of vorticity: (a) *Re=1000,* without smoothing function, (b) *Re=1000*, and (c) *Re=10000* both with smoothing function.

Figure 7 shows the C_d time distribution for *Re=1000* and *Re=10000*. In this case, the simulations were performed with turbulence model and with smoothing function. Comparing Fig. (7) to Figs. (3) and (5) we see that the numerical instability was well controlled. The oscillation that remains at Fig. (7) is of physical nature. To be sure that the mean value of C_d was well calculated, this parameter was compared with others authors for several values of Reynolds number. In order to have good agreements, higher resolution calculation (*250 x 500*) was performed. Table 1 shows the results compared with others experimental and numerical results.

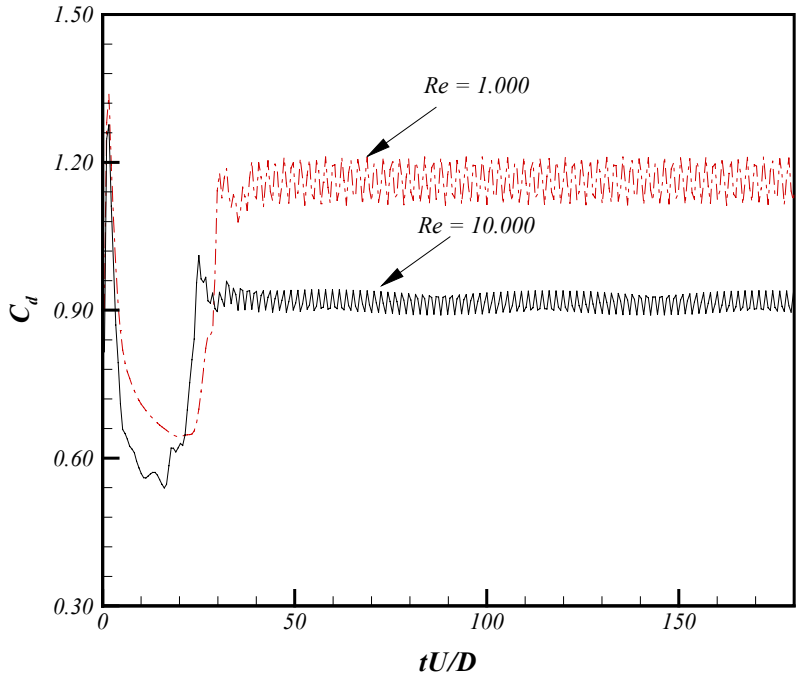

Figure 7. Time evolution of drag coefficient at *Re = 1000* and *Re =10000*. Both calculations with smoothing function and turbulence model.

Table 1. Comparisons of medium values of the drag coefficients.

Re	*Cd*				
	Present work	Braza *et al.* (1986)	Henderson (1997)	Lima e Silva (2002)	Sucker e Brauer (1975)
100	*1.38*	*1.36*	*1.35*	*1.39*	*1.45*
300	*1.22*	-	-	*1.22*	*1.22*
1000	*1.16*	*1.20*	*1.51*	-	*0.96*
10000	*0.91*	-	-	-	*1.10*

4.2. Simulations with rotating cylinder

The flow dynamics of rotating cylinders is different from that observed in stationary cylinders. The rotation can eliminate partially or totally the vortices. Vortices are shedding at low values of specific rotation and disappear completely to $\alpha > \alpha_L$, where α_L is the critical specific rotation. This parameter is defined as:

$$\alpha = \frac{\omega R}{U_\infty}, \tag{8}$$

where R is the cylinder radius and U_∞ is the free stream velocity.

In the present work simulations with rotating cylinders were carried out at Reynolds number *200* and a grid of *300 x 800* points. The domain to these simulations is presented at Fig. 8. The numerical probe shown in this figure is placed at the same position as that used by Carvalho (2003) in his experiments.

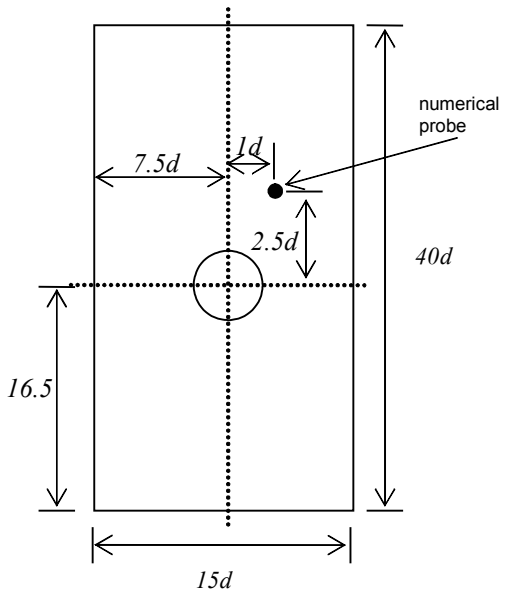

Figure 8. Illustrating scheme of the domain with a rotating cylinder.

4.2.1. Flow visualization

Calculations were performed using the Virtual Physical Model given by Eq. (4). The Lagrangean force field is calculated in such way that the fluid particles at the interface have the same velocity as the cylinder surface.

Figure 9 shows the flow visualization by surfaces of vorticity of the present work and that of Carvalho (2003). It can be observed that the wake is displaced with respect to the vertical symmetry plan as the specific rotation is increased. The numerical results present good agreement with the experimental results of Carvalho (2003).

4.2.2. Strouhal number

Figure 10 presents the time distribution of the lift coefficient over the cylinder and the time distribution of the vertical velocity component obtained by the referred numerical probe illustrated at Fig. (8).

The Strouhal number was obtained by the Fast Fourier Transform (FFT) of the lift coefficient signal and by the velocity that was estoreged by the numerical probe. The results were compared with the numerical results obtained by Badr *et al*. (1989) and the experimental results of Carvalho (2003). The Strouhal number calculated in the present work decreases with the specific rotation. Carvalho's results show an opposite behavior. Table 2 presents comparisons between results of the present work with dates of literature. Table 3, shows the Strouhal number obtained by lift coefficients and the velocity distribution obtained by the numerical probe.

The results of Strouhal number determined using both procedures were similar. Then, the difference observed between the present work and the Carvalho's results isn't due to these methodologies used to calculate the Strouhal number.

Table 2. Strouhal number versus specific rotation.

α	*St*		
	Present work	Carvalho (2003)	Badr *et al.* (1989)
0	*0.1904*	*0.2083*	-
0.5	*0.1866*	*0.2133*	-
1.0	*0.1848*	*0.2166*	*0.2000*
1.5	*0.1825*	*0.2133*	-

Table 3. Strouhal number versus specific rotation, obtained using two procedures

α	St determined using $C_l(t)$	St determined using the numerical probe $u(t)$
0.5	*0.1866*	*0.1852*
1.0	*0.1848*	*0.1847*
1.5	*0.1825*	*0.1821*

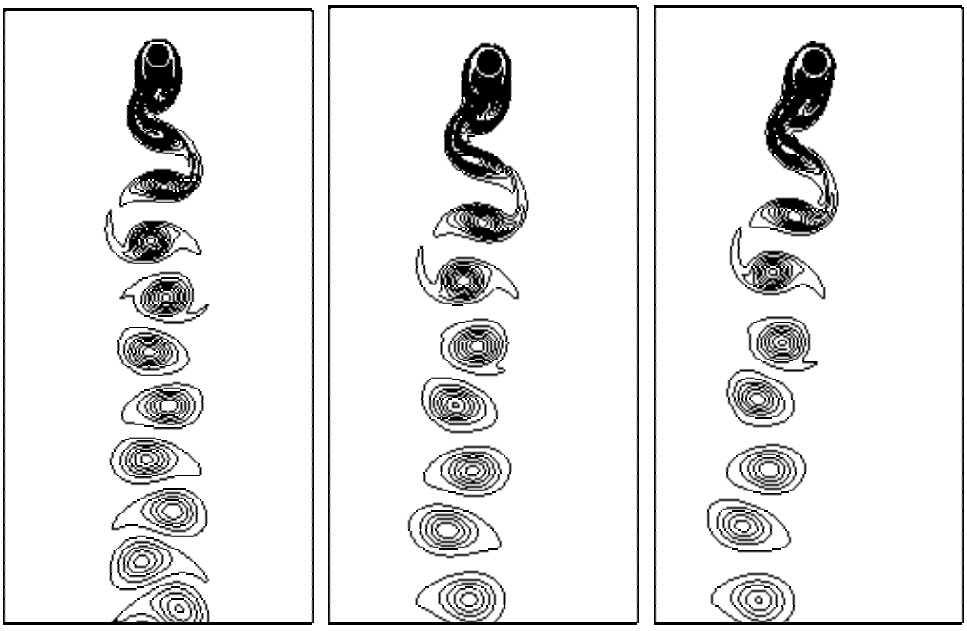

(a) (b) (c)

(d) (e) (f)

Figura 9. Flow visualizations for *Re=200;* present work: (a) α=0.0, (b) α*=0.5*, (c) α*=1.0,* Carvalho (2003): (d) α*=0.0,* (e) α*=0.5* and (f) α *= 1.1*

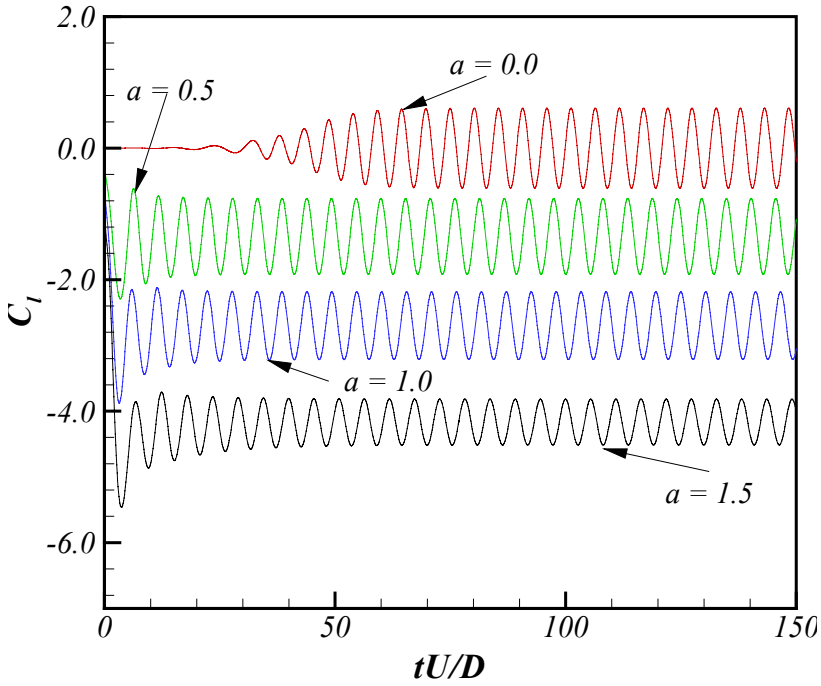

(a)

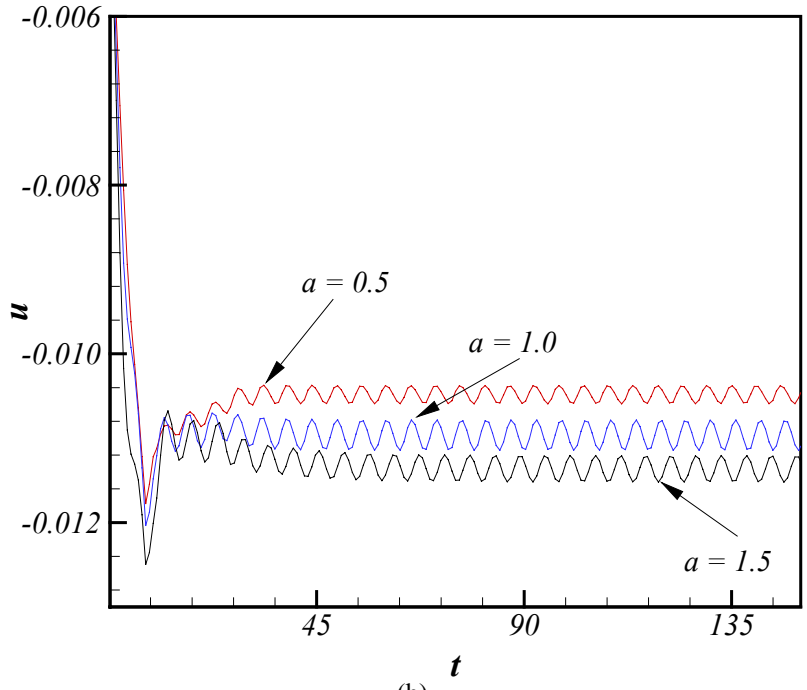

(b)

Figure 10. Time evolution of C_d and vertical component of velocity u for $Re = 200$: (a) lift coefficient, (b) velocity.

5. Conclusions

The use of second order time scheme together with the spatial central scheme is important to the stability of the numerical methodology. As Reynolds number increase, the methodology become instable. Thus, it was necessary the use of turbulence model and the smoothing function. The immersed boundary methodology used in this work is very promising to model and simulate flows over mobile geometries.

6. Acknowledgement

The authors thanks the Conselho Nacional de Desenvolvimento Científico e Tecnológico (CNPq), by the financial support and the School of Mechanical Engineering of the Federal University of Uberlândia.

7. References

Carvalho, G. B., 2003, "Estudo Experimental do Escoamento em torno de Cilindros Circulares em Movimento de Rotação", Dissertação de Mestrado, pp 1-77.

Badr, H. M., Dennis, S. C. R. e Young, P. J. S., 1989, "Steady and Unsteady Flow Past a Rotating Circular Cylinder at Low Reynolds Numbers", Computers & Fluids, Vol. 17, No. 4, pp 579-609.

Braza, M., Chassaing, P. e Minh, H. H., 1986, "Numerical study and physical analysis of the pressure and velocity fields in the near wake of a circular cylinder", J. Fluid Mech., 165, 79.

Fogelson, A. L. e Peskin, C. S., 1988, "A Fast Numerical Method for Solving the Three-Dimensional Stokes' Equations in the Presence of Suspended Particles", Journal of Computational Physics, 79, pp 50-69.

Germano, M., Piomelli, U., Moin, P. and Cabot, W. H., 1991, "A Dynamic Sub-Grid-Scale Eddy Viscosity Model", Phys. Fluids A 3 (7) July, pp. 1760-1765.

Goldstein, D., Handler, R. e Sirovich, L., 1993, "Modeling a No-Slip Flow Boundary with an External Force Field", Journal of Computational Physics, 105, pp 354-366.

Henderson, R. D. (1997), "Nonlinear dynamics and patterns in turbulent wake transition", J. Fluid Mech., 352, 65.

Koopmann, G. H., 1967, "The vortex wakes of vibrating cylinders at low Reynolds numbers", J. Fluid Mech., Vol. 28, part 3, pp 501-512.

Lima e Silva, A. L. F., 2002, "Desenvolvimento e Implementação de uma nova Metodologia para Modelagem de Escoamentos sobre Geometrias Complexas: Método da Fronteira Imersa com Modelo Físico Virtual", Tese de Doutorado.

Lima e Silva, A. L. F., Silveira-Neto A. e Damasceno, J. J. R., 2003, "Numerical Simulation of Two Dimensional Flows over a Circular Cylinder using the Immersed Boundary Method", Journal of Computational Physics, 189, pp 351-370

Peskin, C. S., 1977, "Numerical Analysis of Blood Flow in the Heart", Journal of Computational Physics, 25, pp 220-252.

Saiki, E. M. e Biringen, S., 1996, "Numerical Simulation of a Cylinder in Uniform Flow: Application of a Virtual Boundary Method", Journal of Computational Physics, 123, pp 450-465.

Schneider, G. E. e Zedan, M., 1981, "A Modified Strongly Implicit Procedure for the Numerical Solution of Field Problems", Numerical Heat Transfer, 4, 1.

Silva, A. R., 2004, "Simulação numérica de escoamentos em transição sobre cilindros imersos", Dissertação de Mestrado, pp 1-95.

Silveira-Neto, A., Mansur, S. S., Silvestrini, J. H., 2002, "Equações da turbulência: média versus filtragem", III Escola de Primavera - Transição e Turbulência, UFSC, 1, pp 1-7.

Silveira-Neto, 2003, "Introdução à Turbulência nos Fluidos", Apostila do Curso de Pós Graduação em Engenharia Mecânica, LTCM/FEMEC/UFU.

Smagorinsky, J. 1963, "General Circulation Experiments with Primitive Equations", Mon. Weather Rev., Vol. 91, pp 99-164.

Souza, L. F., Mendonça, M. T., Medeiros, M. A. e Kloker, M., 2002, "Three Dimensional Code Validation for Transition Phenomena", III Escola de Primavera - Transição e Turbulência.

Sucker, D. e Brauer, H., 1975, "Fluiddynamik bei der angestromten Zilindern", Wärme und Stoffubertragung, 8, 149.

Tuszy´nski, J. e Löhner, R., 1998, "Control of a Kármán Vortex Flow by Rotational Oscillations of a Cylinder", pp 1-12.